Increased Ca^{2+} storage capacity of the skeletal muscle sarcoplasmic reticulum of transgenic mice over-expressing membrane bound calcium binding protein Junctate

Alexandra Divet[1], Silvia Paesante[1], Cristiano Grasso[1], Dario Cavagna[1], Cecilia Tiveron[2], Cecilia Paolini[3], Feliciano Protasi[3], Corinne Huchet-Cadiou[4], Susan Treves[5] and Francesco Zorzato [1*]

[1]Department of Experimental and Diagnostic Medicine, Section of General Pathology, University of Ferrara, 44100 Ferrara, Italy. [2]Transgenic Mice Service Center, Experimental Research Center, Regina Elena Institute, 00158 Roma, Italy. [3]Interuniversitary Institute of Myology, CeSI, Center for Research on Aging, University G. d'Annunzio School of Medicine, 66023 Chieti, Italy. [4]UMR CNRS U3B 6204, Faculty of Sciences and Techniques, University of Nantes, 44322 Nantes, France, and [5]Departments of Anesthesia and Research, Hebelstrasse 20, Basel University Hospital, 4031 Basel, Switzerland

Key words: **Junctate, skeletal muscle, transgenic mice, sarcoplasmic reticulum, Ca^{2+} homeostasis**

Running Title: Junctate over-expression in skeletal muscles

*Address correspondence to:
Francesco Zorzato,
Dipartimento di Medicina Sperimentale e Diagnostica, Sez. Patologia Generale,
Università degli Studi di Ferrara,
Via Borsari 46, 44100 Ferrara, Italy.
Tel.: (+39) 0532-291356
Fax: (+39) 0532-247278.
email: zor@unife.it; or fzorzato@uhbs.ch

Total number of figures **7**
Total number of tables **4**

ABSTRACT

Junctate is an integral sarco(endo)plasmic reticulum protein expressed in many tissues including heart and skeletal muscle. Because of its localization and biochemical characteristics, junctate is deemed to participate in the regulation of the intracellular Ca^{2+} concentration. However, its physiological function in muscle cells has not been investigated yet. In this study we examined the effects of junctate over-expression by generating a transgenic mouse model which over-expresses junctate in skeletal muscle. Our results demonstrate that junctate over-expression induced a significant increase in SR Ca^{2+} storage capacity which was paralleled by an increased 4-chloro-*m*-cresol and caffeine-induced Ca^{2+} release, whereas it did not affect SR Ca^{2+}-dependent ATPase activity and SR Ca^{2+} loading rates. In addition, junctate over-expression did not affect the expression levels of SR Ca^{2+} binding proteins such as calsequestrin, calreticulin and sarcalumenin. These findings suggest that junctate over-expression is associated with an increase in the SR Ca^{2+} storage capacity and releasable Ca^{2+} content and support a physiological role for junctate in intracellular Ca^{2+} homeostasis.

(163 words)

INTRODUCTION

Alterations of the intracellular calcium concentration, $[Ca^{2+}]_i$, are involved in numerous cellular functions in excitable as well as non-excitable cells. In many cells, the interaction of ligands with specific receptors present on the plasma membrane coupled to PIP_2 hydrolysis and IP_3 generation, leads to a rapid but transient increase in the cytoplasmic $[Ca^{2+}]$. In view of its role as a second messenger, the free cytosolic $[Ca^{2+}]$ cannot remain elevated for a long period of time and its concentration is tightly regulated by many proteins and organelles. In striated muscles, the sarcoplasmic reticulum (SR) which is a highly specialized form of the endoplasmic reticulum (ER), represents the main intracellular Ca^{2+} storage compartment and plays a key role in excitation-contraction (EC) coupling (for reviews see Melzer et al., 1995; Berchtold et al. 2000). In skeletal muscle, electrical depolarization of the plasma membrane leads to an increase in the myoplasmic $[Ca^{2+}]_i$ which in turn activates the contractile apparatus, leading to muscle contraction a phenomenon known as EC coupling. The anatomical site of EC coupling is the calcium release unit (CRU), a unique intracellular synapse made up by two membrane compartments the extracellular sarcolemma and transverse (T) tubular system, and the sarcoplasmic reticulum (SR) terminal cisternae. The transverse (T) tubular system is an invagination of the sarcolemma into the muscle fibers and its lumen communicates with the extracellular space. CRUs may be formed by the direct association of the SR with the plasma membrane (*peripheral couplings,* mostly found in developing muscles) or by the association of three elements, a central transverse T tubule, and two closely apposed terminal cisternae of the SR (triad, representing mature CRUs). Two macromolecular complexes containing two distinct Ca^{2+} channels are located on the triad and are intimately involved in EC coupling: the voltage-gated Ca^{2+} channel or dihydropyridine receptors (DHPR) localized in T tubule membrane and the ryanodine receptors (RyR), or feet, localized in the SR terminal citernae membranes (Rios et al., 1991; Franzini-Armstrong and Jorgensen, 1994). In skeletal muscle, DHPRs respond to plasma membrane depolarization by sensing the voltage variation and induce Ca^{2+} release from the SR via direct activation of RyRs, independently of extracellular Ca^{2+} (Lamb and Stephenson, 1990; Marty et al. 1994; Nakai et al., 1996). The elevated myoplasmic $[Ca^{2+}]_i$ binds to troponin C thereby allowing actin and myosin to interact and leading to shortening of the sarcomere which leads to contraction of the muscle fiber. Subsequently, rapid reuptake of Ca^{2+} into the SR by the Ca^{2+}-ATPase decreases the myoplasmic $[Ca^{2+}]_i$ leading to muscle relaxation. The

molecular biology, biophysical properties and functional regulation of the major proteins involved in Ca^{2+} homeostasis and EC coupling are now well established and any perturbation in this Ca^{2+} signaling machinery can potentially lead to alterations of cellular functions and diseases (MacLennan, 2000).

The junctional face membrane (JFM), corresponding to the portion of SR terminal cisternae facing the T tubules, is intimately involved in the EC coupling process. Biochemical data indicate that in addition to RyRs, the JFM contains several protein constituents, including triadin, calsequestrin, junctin, histidine rich Ca^{2+} binding protein (HRC), mitsugumin-29, junctophilin, 90 kDa protein or JP-45 (MacLennan and Wong, 1971; Hofmann et al., 1989; Caswell et al., 1991; Jones et al., 1995; Takeshima et al., 1998; Froemming et al., 1999; Takeshima et al., 2000; Zorzato et al., 2000; Anderson et al., 2003). However, the JFM is also endowed with numerous other less abundant proteins having a molecular mass ranging between 20 kDa and 120 kDa (Costello et al., 1986), whose identity and functional role are still obscure. Because of their localization, these proteins are likely to be involved in the EC coupling mechanisms and regulation of intracellular Ca^{2+} homeostasis. During the past decade, several groups have focused their research on the proteomic structure of the longitudinal SR and terminal cisternae: in the present investigation we identified and characterized junctate a novel integral membrane protein of the SR/ER membranes (Treves et al., 2000). Junctate is a 33 kDa protein which is expressed in a variety of tissues including brain, kidney, liver and heart and to a lesser extent in skeletal muscle; it results from alternative splicing of the same gene which generates junctin and aspartyl-ß-hydroxylase (Treves et al., 2000; Dinchuk et al., 2000; Hong et al., 2001). Junctin is an integral SR membrane protein that forms a quaternary complex with the RyRs, calsequestrin, and triadin and has been shown to participate in Ca^{2+} release from heart and skeletal muscle (Jones et al., 1995; Zhang et al., 1997). Different isoforms of aspartyl-ß-hydroxylase can be generated by alternative splicing of the COOH-terminal tail however the full length isoform has enzymatic activity and catalyses the addition of hydroxyl groups to particular Asp or Asn residues within cEGF domains of numerous proteins (Gronke et al., 1990; Wang et al., 1991). The biological function(s) of this hydroxylation however, has yet to be defined.

Our research has focused on the biochemical properties and physiological role of junctate: we have demonstrated that this protein contains a negatively charged COOH-terminal domain

which is located in the lumen of the ER and confers to the protein the ability to bind Ca^{2+} (Treves et al., 2000). We have also shown that junctate is intimately involved in Ca^{2+} homeostasis because its NH_2-cytoplasmic domain can directly interact with the IP_3R and the TRPC3 cationic plasma membrane channel thereby increasing the local Ca^{2+} concentration in subdomains of the ER (Treves et al., 2004). In order to evaluate the functional role of junctate in the regulation of Ca^{2+} homeostasis and its potential involvements in the EC coupling mechanisms, we generated a model of transgenic mouse over-expressing junctate in skeletal muscles. Our results demonstrate that this over-expression results in increased SR Ca^{2+} storage capacity and an increase in releasable Ca^{2+}, adding strong evidence in support of the physiological functions of junctate *in vivo*.

MATERIALS AND METHODS

Generation of transgenic mice

The transgene was constructed inserting the human junctate cDNA sequence (Treves et al., 2000) downstream to the tissue-specific α-actin promoter to target expression to skeletal muscle (Greenberg et al., 1994) followed by the poly(A)-SV40 poly-adenylation signal (Fig. 1A). The different fragments of the construct were PCR amplified using specific primers and then consecutive steps of digestion of p-Bluescript II KS(-) 3.0 kb plasmid, insertion of fragments, ligation and cloning. The transgene construct was liberated from the plasmid vector by digestion with XhoI and EcoRI restriction enzymes. Construct was verified by sequencing and then the purified DNA fragments were used to generate the transgenic animals.

A colony of transgenic mice (TG) was established in the Transgenic Mice Service Center (Roma, Italy) using the pronuclear DNA injection of single-cell embryos approach. Briefly, fertilized ova were collected and a DNA solution containing several copies of the transgene construct was injected into the egg's pronuclei leading to the head-to-tail integration into the genome of several copies of the transgene. After one cell division cycle, the resulting embryos were placed into the oviduct of a pseudopregnant female. This approach allowed us to introduce the transgene in the genome of whole animal and it was stably passed on to its progeny. The line was maintained by backcrossing TG with C57BL/6 animals. Heterozygous mice obtained from 1 backcross in C57BL/6 were used for intercross breeding to generate homozygous transgenic littermates. Homozygous mice were healthy and fertile and three lines TG mice were generated and characterized to exclude problems arising from the random insertion of the transgene into a specific gene. All animals were genotyped at weaning by standard PCR procedure using genomic DNA extracted from tail biopsies and amplified using two pairs of primers (F1 5'-ACCTGCCAGCAGTACTTTTC-3', F2 5'-CAAAGCATGGAGGACACAAGAATG-3', R 5'-AATAAAACTTTGGCATCATCCACATCAAAATCTCC-3') specific for human junctate yielding fragments of 259 bp and 358 bp. All PCR reactions were performed in a Perkin Elmer 9600 thermocycler using previously described amplification conditions (Treves et al., 2000). Southern blot analysis was also performed to confirm the genotype of the mice. Briefly, genomic DNA was digested with HindIII and probed with 897 bp [^{32}-P]-dATP labeled cDNA fragment. Hybridization

was performed overnight at 42°C in a shaking waterbath. The membrane was washed 3 times at high stringency (65°C in 0.2X SSCP, 0.1% SDS) air dried and autoradiography performed (Treves et al., 2000). All experiments were performed on male age-matched (3 month old) homozygous transgenic and wild type mice. The experiments with TG and wild type (WT) animals were approved by the Ethical Committee of the University of Ferrara.

Isolation of SR membranes

SR vesicles were prepared as described previously (Saito et al., 1984); briefly, hindlimb and back muscles were excised, trimmed of excess fat and connective tissue and then immediately homogenized in a buffer (homogenization buffer) containing: 250 mM sucrose, 10 mM HEPES, 0.5 mM phenylmethyl-sulfonyl fluoride, 1 mM benzamidine, 1 mM iodoacetamide and 1.5 μM pepstatine, pH 7.4. The muscle homogenate was centrifuged for 15 min at 1,000 x g (RC-5B Sorvall centrifuge, using a SS34 rotor). The supernatant was centrifuged at 12,000 x g (Sorvall centrifuge, SS34 rotor) for 15 min. Then, the supernatant was collected and centrifuged for 60 min at 100,000 x g (Beckman L8-70M ultracentrifuge). 100,000 x g pellet containing SR membranes was resuspended in homogenization buffer and flash frozen in liquid nitrogen and stored at -80°C until use. Protein concentration was determined using the DC Proteins Assay kit (Bio-Rad) and bovine serum albumin as a standard.

Antigenic peptide synthesis and preparation of anti-junctate antibodies

Polyclonal antibodies were generated by immunizing a New Zealand white rabbit, with a synthetic peptide designed on a sequence derived from the NH_2-terminal of human junctate. Two hundred micrograms of MAP peptide (MAEDKETKHGGHKNGRK) were emulsified with MPL-TDM adjuvant and used to immunize a rabbit as previously described (Anderson et al., 2003). IgG's were purified from serum by protein A chromatography as previously described (Treves et al., 2000; Anderson et al., 2003) and their immunoreactivity determined by Western blot analysis.

Electrophoresis and immunological staining

All western blot analysis were performed on the total SR microsomal fraction isolated from skeletal muscle of WT and TG mice. SDS-PAGE, protein transfer onto nitrocellulose membranes

and immunostaining were carried out as previously described (Treves et al., 2000). Proteins were visualized by Ponceau red staining or by Coomassie Brilliant Blue staining. Blots were probed with anti-skeletal calsequestrin antibodies, anti-sarcalumenin antibodies (1:2000, Santa Cruz), anti-calreticulin antibodies (1:1000, Santa Cruz), anti-SERCA1 antibodies (1:500, Santa Cruz), anti-SERCA2 antibodies (1:5000, Santa Cruz) or with rabbit anti-junctate antibodies for 1 hour in TBST followed by incubation with peroxidase-labeled protein G. The reaction was developed using chemiluminescence kit (Roche diagnostic) and bands visualized by autoradiography and digitally acquired using an Epson or a Microtek scanner. Figures were assembled using Adobe Photoshop or Corel Draw. To quantify and compare the protein levels between wild type and transgenic samples, densitometric analysis of bands was performed using the NIH image 1.63 software.

Measurement of Ca^{2+} loading rate and Ca^{2+} release from SR vesicles

Ca^{2+} loading was continuously monitored by following differential absorbance change of the Ca^{2+} indicator Antipyrylazo-III at 710-790 nm in a Beckman DU-7400 spectrophotometer (Mitchell et al., 1983; Zorzato et al., 1985). Ca^{2+} flux, net Ca^{2+} loading and Ca^{2+} release, were continuously monitored spectrophotometrically (Palade, 1987).

Single cell $[Ca^{2+}]_i$ measurements

Myotubes were obtained from the hindlimb muscles of newborn mice by enzymatic dissociation, plated on laminin-coated glass coverslips and allowed to grow in Ham's F-10 (Invitrogen) medium supplemented with 20% fetal bovine serum, antibiotics and 2 ng/ml bFGF overnight; after 24 hours the medium was changed to Ham's F-10 plus 20% fetal bovine serum, antibiotics and 5 ng/ml bFGF and the cells were allowed to proliferate until they reached 50-60% confluency; medium was then switched to differentiation medium (Dulbecco's MEM plus 5% horse serum and antibiotics) upon which cells started to fuse into multinucleated myotubes (usually day 3 or 4). Once the cells were differentiated, they were loaded with the fluorescent Ca^{2+} indicator fura-2 and single cell intracellular calcium imaging was performed as previously described (Ducreux et al., 2004). Coverslips were mounted onto a 37°C thermostatically controlled chamber which was continuously perfused with Krebs Ringer medium; individual cells were stimulated with a 12-way 100 mm diameter quartz micromanifold computer controlled microperfuser (ALA Scientific) as

previously described; the agonist (4-chloro-*m*-cresol, 4-CmC) or caffeine were dilutes to the final concentration in Krebs-Ringer containing contaminating calcium + 100 µM La^{3+} to block influx from the extracellular medium; Ducreux et al., 2004).

To measure Ca^{2+} influx, intracellular stores were depleted by loading cells with 5 µM fura-2 in the presence of 1 mM EGTA at 37°C for 60 minutes. Coverslips were mounted and cells continuously perfused with Krebs-Ringer containing 0.5 mM EGTA and no added Ca^{2+}. Ca^{2+} influx was investigated in individual cells by perfusing them with Krebs-Ringer containing 2 mM Ca^{2+}. On-line (340 nm, 380 nm and ratio) measurements were recorded using a fluorescent Axiovert S100 TV inverted microscope (Carl Zeiss GmbH, Jena, Germany) equipped with a 20x water-immersion FLUAR objective (0.17 NA), filters (BP 340/380, FT 425, BP 500/530) and attached to a Hamamatsu multiformat CCD camera. The cells were analyzed using an Openlab imaging system and the average pixel value for each cell was measured at excitation wavelengths of 340 and 380 nm.

Measurement of Ca^{2+}- dependent ATPase activity

ATPase rate was assessed by a spectrophotometric enzyme-coupled assay as described previously (Warren et al., 1974; Zorzato et al., 1985). The basal ATPase rate was measured in the presence of 0.2 mM EGTA and the total ATPase rate, after the addition of 0.2 mM $CaCl_2$ ($[Ca^{2+}]$ estimated at 10 µM). The Ca^{2+}-dependent ATPase activity was calculated as the difference between total and basal ATPase activity. Maximal Ca^{2+}-dependent ATPase rate was obtained in the presence of the Ca^{2+} ionophore A23187 (1.5 µg.mL^{-1}).

Experimental protocol with skinned-fibers

Fast-twitch (*extensor digitorum longus*, EDL) and slow-twitch (*soleus*) muscles were dissected from WT and TG. Small bundles of two to five fibers were isolated manually from tendon to tendon from both freshly-isolated muscles and, with the aid of a microscope, short portions (100-250 µm in diameter; 2-3 mm in length) were excised. Chemical skinning was carried out immediately after dissection, using Triton X-100. Skinned fibers were transferred to a chamber and mounted between two stainless-steel tubes that supported a metal target facing the sensor of a transducer, as previously described (Divet and Huchet-Cadiou, 2002; Divet et al., 2005). At the

beginning of each experiment, the fiber was adjusted to a length where it was slack, and then stretched progressively until at pCa 4.5 whether the tension developed reached its peak (which was generally equals to the resting length plus 20%). All experiments were performed at 22°C.

In order to solubilize the sarcolemma and SR membranes, muscle fibers were incubated at room temperature for 1 h in a relaxing solution (pCa 9.0, see composition below) containing 1% Triton X-100 (v/v), and then washed several times in detergent-free relaxing solution. Following this skinning step, fibers were stored at -20°C in relaxing solution containing 50% glycerol (v/v). Tension/pCa relationships (pCa = $-\log_{10}$ $[Ca^{2+}]$) were obtained by exposing Triton-skinned fibers sequentially to solutions with decreasing pCa values until the maximum tension (Tmax) was reached (at pCa 4.5), after which fibers were returned to a low $[Ca^{2+}]$ (pCa 9.0). The isometric tension was recorded continuously using a chart recorder and the baseline tension was established at the steady-state measured in relaxing solution. To obtain the Ca^{2+}-sensitivity curve, data for the relative tension (T/Tmax) were fitted with a modified Hill equation (Huchet and Leoty, 1993) $T/Tmax = [Ca^{2+}]^{nH} / (K^{nH} + [Ca^{2+}]^{nH})$, where K is the $[Ca^{2+}]$ at which activation reached half of its maximum value. pCa_{50}, the negative logarithm to base 10 of K, is a measure of the apparent Ca^{2+}-sensitivity of contractile proteins, and the Hill coefficient (n_H) is an estimate of the degree of cooperativity. These two parameters were calculated for each experiment using linear regression analysis. n_H was calculated for each fiber as the slope of the fitted straight lines. The tension obtained at each $[Ca^{2+}]$ was normalized for the cross-sectional area of the fiber.

The composition of skinned-fiber solutions was calculated according to Godt and Nosek (1989). The relaxing (pCa 9.0) and activating (pCa 4.5) solutions consisted of: 10 mM EGTA, 30 mM imidazole, 30.6 mM Na^+, 1 mM Mg^{2+}, 3.16 mM MgATP and 12 mM phosphocreatine (pH 7.1) The ionic strength of these solutions was 160 mM. Solutions containing intermediate values of $[Ca^{2+}]$ were obtained by mixing the pCa 9.0 and pCa 4.5 solutions in appropriate proportions. Similarly, solutions containing different concentrations of Sr^{2+} were used to study tension/pSr relationships (pSr = $-\log_{10}[Sr^{2+}]$).

Electron microscopy

a - Preparation of samples of Electron Microscopy (EM). EDL and Soleus muscle were carefully dissected from TG and WT mice. After gentle stretch, muscles were pinned tendon-to-tendon on a

sylgard dish and fixed at room temperature in 3.5% glutaraldehyde diluted in 0.1 M sodium cacodylate buffer, pH 7.2 for 2h (fixative solution). Fixed muscles were stored at 4°C in fixative solution till the embedding procedure. Small bundles of fibers were then post-fixed in 2% OsO_4 in NaCaCo buffer for 2 hr and block stained in saturated uranyl acetate at 60°C for 4 hr. After dehydration in a graded series of ethanol solutions followed by acetone, specimens were embedded in an epoxy resin (Epon 812). Ultrathin sections (about 30-40 nm thick) were cut both longitudinally and transversally in a Leica Ultracut R microtome (Leica Microsystem, Austria) using a Diatome diamond knife (DiatomeLtd. CH-2501 Biel, Switzerland). Sections, after staining in 4% uranyl acetate and lead citrate, were examined with a FP 505 Morgagni Series 268D electron microscope (Philips), equipped with Megaview III digital camera.

b - Quantification of mitochondria and CRUs. The density of triads and mitochondria were determined by counting their number in EM images from 5-6 different fibers for each specimen. In each fiber 10 micrographs - all at the same magnification (11,000 X) and with no overlapping regions - were randomly collected from longitudinal sections, for a total of 50 to 60 electron micrographs for each muscle. Triads and mitochondria were marked and counted in each micrograph. Note that only those structures formed by the association of SR and T tubules and that contains RyRs were identified as CRUs. The results of the CRUs and mitochondria counting are presented in Table 3 as n. of junctions/100 μm^2 of sectional area ± standard deviation (SD). On the other hand, the number of peripheral couplings is given as n. of junctions/100 μm of linear length of surface membrane. In the latter case, at least 600 μm of surface membrane were closely analysis in each of the 6 fibers analyzed in each specimen.

c - Measurement of the average width of SR lumen. The width of the SR/T tubule junctional gap was calculated from measurements obtained in a different set of micrographs taken at 22,000 X (or higher) magnification. Measurements were taken measuring the linear distance between the two internal leaflet of the SR terminal cisterna membrane (as shown in the detail of Fig. 5A). A total of 152 to 231 SR terminal cisternae were measured in each muscle and the results of these measurements are collected in Table 3, column III.

d - Statistical Analysis. Means ± standard deviations (SD) were determined from individual data values by descriptive statistics using Microsoft Office Excel 2003. To evaluate the differences between different groups, the data were compared by analysis of variance (ANOVA) and Student's

t test. Values of P < 0.05 (95% confidence) were considered significant.

Statistical analysis

Data were analyzed using the Student's *t* test for unpaired samples. A value of $P < 0.05$ was considered significant. Data are expressed as mean ± SEM with the number of observations.

RESULTS

Genotyping of transgenic mice over-expressing junctate

Figure 1A shows a schematic representation of the construct which was used to obtain transgenic animals over-expressing human junctate. Based on the expression of the transgene, three lines of mice were selected and animals were genotyped at weaning by standard PCR procedure using genomic DNA and two pairs of specific primer sequences (product length 259 bp and 358 bp; approximate location indicated on the junctate cDNA sequence of panel A). WT and TG mice were identified (Fig. 1, panel B) and Southern blot analysis using a probe encompassing 897 bp of human junctate cDNA, was performed to confirm stable genomic integration of the transgene and corroborate the genetic status of the mice (Fig. 1, panel C).

Expression and localization of junctate in transgenic mice

The transgene insertion in genomic DNA does not necessarily prove the existence of a protein product. We approached this issue by performing western blot analysis on the total SR microsomal fraction isolated from the skeletal muscles of WT and TG animals. Anti-junctate antibodies raised against the first 17 NH_2-terminal residues of the human junctate protein do not recognize the mouse isoform of junctate; therefore the immunopositive band in figure 1 D and E is directly linked to the quantity of junctate TG expression. In order to confirm the specificity of the 33 kDa immunoreactive band, competition experiments were performed incubating the antibodies with increasing amounts of the competing MAP peptide which was used to immunize the rabbit. The results depicted in figure 1E demonstrate that the immunological reactivity of the anti-junctate antibodies was specific for human junctate as it was proportionally diminished by the addition of the competing peptide used as antigen. These results confirm the expression of the transgene at the protein level in skeletal muscles and substantiate the validity of our TG model (Fig. 1, panel D)

Calcium homeostasis in SR from TG and WT mice

In order to investigate the functional effect of its over-expression in skeletal muscle SR, we determined Ca^{2+} storage and Ca^{2+} release capacity of sarcoplasmic reticulum from skeletal muscles of WT and TG mice in intact muscle cells and in isolated SR vesicles.

Ca^{2+} homeostasis in intact muscle cells was investigated by isolating myotubes from WT and TG mice, Figure 2 A shows a typical trace obtained after stimulating a myotube from a WT (____) or TG mouse (……) with 600 µM 4-CmC; typically junctate over-expressing cells exhibited a larger Ca^{2+} transient than myotubes from wild type animals. Figure 2B shows that the increased Ca^{2+} release was significantly larger when cells were stimulated with either 4-chloro-*m*-cresol or caffeine, substantiating that over-expression of junctate leads to a larger amount of Ca^{2+}which could be released from the SR by RyR pharmacological activation. Since in non-muscle cells, we demonstrated that junctate couples Ca^{2+} release and influx from the extracellular environment (Treves et al., 2004), we also investigated if the over-expression of junctate also affected Ca^{2+} influx stimulated by store depletion. Myotubes were depleted of Ca^{2+} by loading them in Krebs-Ringer containing 1 mM EGTA and in the presence of 5 µM fura-2. Such cells exhibit a lower resting [Ca^{2+}] than normal myotubes (compare the fluorescence ratio of cells in figure 2A and 2C) and upon addition of 2 mM Ca^{2+}, show a typical increase in cytoplasmic [Ca^{2+}]; junctate over-expressing cells exhibited a Ca^{2+} influx transient which was significantly larger than that observed in myotubes isolated from WT mice (fig. 2D). Altogether these results indicated that the over-expression of junctate results in an increase of the SR Ca^{2+} storage capacity, in an increase of the Ca^{2+} released by RyR1 agonists 4-CmC and caffeine and in a larger Ca^{2+} influx observed after depletion of intracellular Ca^{2+} stores.

Calcium fluxes were also examined in cell- free system by using isolated SR vesicles. Figure 3A shows typical traces obtained when microsomal preparations from 3 months old WT and TG were loaded with several pulses of $CaCl_2$. The amount of Ca^{2+} which could be loaded into the SR of TG mice was always higher than that loaded into the SR of WT mice (mean number of pulses was 9 and 7 for TG and WT, respectively). Note that the same end point level of Ca^{2+} loading was reached in vesicles from WT and TG mice and that additional pulses of Ca^{2+} would result in Ca^{2+} induced Ca^{2+} release. At the end of the experiments the Ca^{2+} ionophore A23187 (5 µg.mL^{-1}) was added to release all the Ca^{2+} accumulated in the SR vesicles (Fig. 3, panel A). Our results demonstrate that both maximal Ca^{2+} loading (Fig. 3B) as well as the total amount of Ca^{2+} released by the Ca^{2+} ionophore A23187 (Fig. 3C), were significantly increased by approximately 21%, in TG mice compared to their WT counterpart. Similar results were obtained using another junctate over-expressing TG mouse line (results not shown).

We next investigated whether the Ca^{2+} pool which was increased in the TG animals, was endowed with the RyR1 by activating Ca^{2+} release with 4-chloro-*m*-cresol (4-CmC), a potent and specific activator of RyR1 (Zorzato et al., 1993; Herrmann-Frank et al., 1996). SR microsomes were preloaded with Ca^{2+} to maximal capacity and then Ca^{2+} release was activated by the addition of 100-2500 µM 4-CmC (Fig. 4). Under these conditions, the maximal extent of Ca^{2+} release was significantly increased in SR vesicles derived from TG mice compared to their WT counterparts (Fig. 4). Indeed, both the maximal extent of Ca^{2+} release as well the EC_{50}, were significantly increased (Student's *t* test $P<0.01$) in SR preparations from TG mice compared to those from WT (Fig. 4 and Table 1). This was not due to major change in the expression level of the RyR1 protein as shown by [^{3}H]-ryanodine experiments since at 5 nM the amount of ligand bound to the high affinity site in the total SR microsomes from TG and WT mice was 0.466 and 0.44 pmol/mg SR protein, ($P<0.6$) respectively. Over-expression of the lumenal calcium binding protein narrowed the concentration range for 4-CmC induced calcium release. As shown in Figure 4 the extent of Ca^{2+} release triggered by saturating concentrations of 4-CmC was higher in microsomes from TG mice, the 4-CmC EC_{50} was shifted to the right, and the cooperativity of the of Ca^{2+} release induced by 4-CmC was increased in SR preparations from TG mice (Table 1).

In order to verify whether this increase in Ca^{2+} storage capacity was directly linked to the presence of junctate acting as a lumenal Ca^{2+} buffer, rather than an enhanced SR Ca^{2+}-ATPase activity of the isolated SR vesicles, we performed experiments to study the activity and expression of the SR Ca^{2+}-ATPase. Our results demonstrate that neither the maximal turn-over rate of Ca^{2+}-dependent ATPase nor Ca^{2+} loading rates differed between WT and TG mice (Table 2). Western blot analysis of SR proteins from total microsomal fraction of WT and TG mice confirmed that the expression of both isoforms of SR Ca^{2+}-ATPase, SERCA1 and SERCA2, was similar between junctate over-expressing and wild type mice (Fig. 5). The next set of experiments were performed to exclude that the increase in calcium loading in isolated sarcoplasmic reticulum from TG mice over-expressing junctate (Treves et al., 2000) could be ascribed, at least in part, by changing in the expression of other known sarcoplasmic reticulum Ca^{2+} binding proteins. We focused on the expression of calsequestrin, the major SR luminal Ca^{2+} binding protein, but also on other less abundant proteins such as sarcalumenin and calreticulin. The level of expression of these Ca^{2+} binding proteins in total SR fraction isolated from TG mice was not modified compared to their WT

counterpart (Fig. 5).

The increased calcium storage capacity of the sarcopasmic reticulum membrane network of intact fibers should be associated with an increase in calcium cycling within muscle fibers. We reasoned that in order to sustain the increase of calcium cycling, adaptive responses of the subcellular structures may occur. To address this issue we next performed electron microscopy ultrastructural analysis of WT and TG skeletal muscles.

Electron microscopy

Ultrastructural analysis performed by electron microscopy (EM) on (*extensor digitorum longus*) EDL and Soleus muscles indicates that junctate over-expression does not induce drastic alterations in the general organization and architecture of muscle fibers (Fig. 6). In both muscles types, we analyzed qualitatively and quantitatively the overall ultrastructure of contractile, EC coupling, and mitochondrial apparatuses. Contractile and EC coupling apparatuses appear to maintain their normal organization even in TG mice, i.e. myofibrils appear to be well aligned with one another (Fig. 6, Z lines), while triads are correctly positioned and oriented at the transition between the I and the A bands (Fig. 6, small arrows). Analysis at a higher magnification (Fig. 6, see details), shows that the triads in TG mice are not visibly different from the triads found in muscles from WT mice: they are formed by three elements, two SR vesicles closely apposed to a central T tubule, and contains two rows of feet, or RyRs, in the junctional gap between the two membranes (small arrows in the enlarged details). Measurements of the SR lumen width in WT and TG mice did not reveal significant differences and supported the idea that the triad structure is not significantly altered (see Table 3, column II).

The only noticeable alteration detected by EM analysis concerns the content of mitochondria in the EDL muscle (Fig. 6, empty arrows). In the EDL from junctate TG mice we found a large increase in the total number of mitochondria when compared to WT (49.3 ± 14.3 vs 30.9 ± 10.7 per 100 μm^2 in transgenic and WT fiber, respectively). In the Soleus, on the other hand, the mitochondrial content remains quite similar in the two specimens (52.4 ± 16.7 vs. 58.9 ± 20.4 per 100 μm^2 of transgenic and WT fiber, respectively). The number of mitochondria in the junctate TG EDL muscle closely matches that of Soleus muscles. Because of this alteration detected in EDL, we looked more carefully at the frequency of both internal triads and peripheral couplings in this

muscle. While we did not find any significant variation in the frequency of peripheral junctions (Table 3, column III), the number of triads appeared to be slightly lower in TG fibers compared to WT fibers: 73.8 ± 17.9 vs. 84.4±16.3 per 100 μm^2 (Table 3, column I). This difference was statistically significant at the Student's *t*-test, P value<0.05.

The increase number of mitochondria visualized at the EM analysis could be linked either to an adaptation of the energy metabolism to the increase of calcium cycling in sarco-tubular membranes or to a fast/slow fiber type transition. To address this issue we examined contractile properties of *extensor digitorum longus* (EDL) and soleus from TG and WT mice.

Over-expression of junctate does not modify the calcium sensitivity of contractile proteins and does not induce fiber type transition

The contractile properties of fast-twitch EDL and slow-twitch soleus skeletal muscles were investigated in Triton X-100 skinned fibers from WT and TG mice (Fig.7). Several parameters were studied such as maximal Ca^{2+}-activated tension (Tmax), the apparent Ca^{2+} sensitivity (pCa_{50}) and the degree of cooperativity in development of Ca^{2+}-activated force (n_H). The results presented in Table 4 indicate that the Tmax generated by contractile apparatus, were not significantly different between WT and TG. Moreover, the Ca^{2+} sensitivity and the Hill coefficient (n_H) were similar for both groups of animals (Table 4A).

Sr^{2+} is a tool to study the properties of contractile protein and particularly to investigate fast to slow transition and studies have shown that skeletal muscle fibers display striking differences with respect to activation of contractile characteristics in the presence of Ca^{2+} vs. Sr^{2+} as the activating ion (Fink et al., 1986; Schiaffino et al., 1996). The results depicted in figure 7 and Table 4 confirm that EDL and soleus fibers exhibit a dissimilar tension/pSr relationship, illustrated by changes in pSr_{50} and n_H values. In addition, the value corresponding to the difference between pCa_{50} and pSr_{50} was significantly different between both types of muscles and this parameter is currently used to differentiate fast- and slow-twitch fibers (Table 4B). However the results we obtained using muscle fibers from TG mice, show that the Sr^{2+} sensitivity and n_H values were similar to those obtained for WT mice, excluding a fast to slow transition induced by over-expression of junctate in skeletal muscle.

DISCUSSION The SR of TG animals shows enhanced Ca^{2+} storage capacity but this is not due to the altered expression of SR Ca^{2+} binding proteins

14/3/2007 17:13
Deleted: .

We previously demonstrated that over-expression of junctate, a high capacity, moderate affinity Ca^{2+} binding protein in COS-7 and HEK293 cells, increases the local Ca^{2+} releasing capacity of the endoplasmic reticulum domains endowed with IP3 receptor calcium channels (Treves et al., 2000, 2004). In the present investigation our aim was to confirm and extend these results using an animal model to demonstrate that *in vivo* junctate can act as calcium storage protein of intracellular calcium stores. We focused our studies on the effect(s) of stable over-expression of junctate on the SR Ca^{2+} loading properties. Interestingly, our data demonstrate that myotubes from junctate over-expressing mice as well as isolated SR microsomes from junctate-overexpressing mice exhibit a significant increase in the Ca^{2+} loading and Ca^{2+} storage capacity compared to their wild type counterparts. These findings are consistent with other investigations in which the effect of over-expression of SR/ER high capacity low affinity Ca^{2+} binding properties was studied. Indeed chronic over-expression of calsequestrin, the major Ca^{2+} binding protein in striated muscle in cardiomyocytes, increased the Ca^{2+} storage capacity of the SR but did not affect the expression level of SERCA or phospholamban (Jones et al., 1998; Sato et al., 1998; Knoollmann et al., 2000; Miller et al., 2005). Consistent results showing an increase in the lumenal SR Ca^{2+} buffering capacity were obtained when the luminal histidine-rich Ca^{2+} binding protein (HRC) was over-expressed in neonatal and adult rat cardiomyocytes (Kim et al., 2003; Fan et al., 2004). Similar results were also described when calreticulin was over-expressed in HeLa cells and *Xenopus* oocytes (Bastianutto et al., 1995; Xu et al., 2000). Furthermore, over-expression of other known calcium storage proteins such as calsequestrin and histidine rich Ca^{2+} binding protein leads to an increase in caffeine-induced Ca^{2+} release (Jones et al., 1998; Sato et al., 1998; Miller et al., 2005; Kim et al., 2003; Fan et al., 2004). Over-expression of junctate also occurs in a membrane compartment endowed with the RyR Ca^{2+} release channel, since we found that (i) direct stimulation of isolated myotubes with either caffeine or 4-CmC resulted in a significantly larger Ca^{2+} transient and (ii) total SR microsomes from transgenic mice show a 24% increase of the extent of calcium release induced by 4-CmC. The over-expression of junctate makes the RyR channel sensitive to a narrower concentration range of RyR agonist 4-chloro-*m*-cresol. Although our data do not provide specific evidence as to the exact mechanisms responsible for the increase of cooperativity of

channel activation by 4-chloro-*m*-cresol, it is temping to speculate that the presence of the lumenal calcium binding protein may play a role in adjusting the sensitivity of the RyR to the agonist, by interfering with lumenal regulatory sites which interact with auxiliary RyR proteins.

Chronic tissue specific protein over-expression, such as that induced in transgenic animal models, might be associated with a set of adaptive events. In particular, it may be possible that a chronic increase of the sarco(endo)plasmic reticulum calcium load of muscle fiber from junctate transgenic skeletal muscle might be linked to integrated adaptive events leading to a reorganization of the molecular composition of the membrane compartment involved in calcium storage. In this case it would be difficult to discriminate between the contribution of the over-expressed protein versus the effect linked to changes of the molecular components of the intracellular calcium store on the Ca^{2+} storage capacity and releasable Ca^{2+} content of sarcoplasmic reticulum. Surprisingly in the junctate over-expressing transgenic animals the levels of expression the major calcium binding proteins of the skeletal muscle sarcoplasmic reticulum membrane, were unchanged. We believe that this study (i) unambiguously demonstrates that junctate plays an important role in the regulation of the lumenal Ca^{2+} level and (ii) supports the conclusion that junctate is a new member of the group of luminal Ca^{2+} binding proteins including calsequestrin, calreticulin, sarcalumenin and calnexin which are involved in regulating the lumenal Ca^{2+} level.

Adaptive response of skeletal muscle from junctate transgenic mouse

An interesting result emerging from this study is that the enhancement of both calcium storage and 4-chloro-*m*-cresol release from sarcoplasmic reticulum is associated with an increase in the number of mitochondria in fast twitch EDL muscle. The number of mitochondria from the EDL of transgenic mice is similar if not identical to that of slow twitch muscles. It is unlikely that such changes in the subcellular composition of EDL from transgenic mice results in a fast to slow fiber transition since skinned fiber experiments clearly demonstrate that the contractile properties of EDL from transgenic mice are not different from those of their wild type counterpart. Fast twitch muscles are characterized by calcium transients which display larger amplitudes and faster kinetics compared to those seen in slow twitch muscle fibers. Most likely the increase in the number of mitochondria in fast twitch muscles is part of an integrated adaptive response to an increase of the energy expenditure required to cope with the chronic increase of calcium cycling across

sarcoplasmic reticulum membrane evoked by the presence of additional lumenal calcium bound to junctate. The mitochondria appear to be localized in the space between myofibril in the same subcellular region enriched in SR membranes. The localization of the mitochondria close to the calcium store might be relevant to the stimulation of mitochondrial metabolism via calcium dependent dehydrogenase of the Krebs cycle which ultimately results in the production of the substrate for the Ca^{2+}-ATPase whose activity is crucial to pump calcium back into sarcoplasmic reticulum lumen. We also cannot exclude the possibility that the larger number of mitochondria might affect the [Ca^{2+}] proximal to the calcium release unit and thus modulate calcium dependent RyR activity. The modulation of RyR activity might control the extent of calcium release from calcium release unit having a higher level of lumenal calcium bound to calcium binding protein junctate.

In conclusion, our data clearly demonstrate that junctate participates in the Ca^{2+} storage and Ca^{2+} release processes and must be considered among the accessory Ca^{2+} binding proteins that might play a physiological role in the regulation of Ca^{2+} homeostasis in both excitable and in non-excitable cells. The fact that junctate is less abundant than other SR Ca^{2+} binding proteins such as calsequestrin, suggests that it may act as a Ca^{2+} regulatory buffer and may be involved in particular physiological and pathophysiological conditions.

ABBREVIATIONS

The abbreviations used are: 4-CmC, 4-chloro-m-cresol; CRU, calcium release unit; DHPR, dihydropyridine receptors; EC, excitation-contraction; EDL, *extensor digitorum longus*; EM, electron microscopy; ER, endoplasmic reticulum; HRC, histidine-rich Ca^{2+} binding; IP3R, inositol triphosphate receptors; JFM, junctional face membrane; PCR, polymerase chain reaction; RyR, ryanodine receptors; SR, sarcoplasmic reticulum; TRPC, transient receptor potential channels; T tubule, transverse tubule; TG junctate transgenic mouse; WT wild type mouse.

ACKNOWLEDGMENTS

This work was supported by grants from the European Union HPRN-CT-2002-00331, from the Schweizereische die Erforschung der Muskelkrankheiten, from F.I.R.B RBAU01ERMX and from the Department of Anesthesia, Basel University Hospital, GGP05025 from Telethon Italy. This study was also supported by a) research grant # GGP030289 from the Italian Telethon Foundation and by b) Research Funds from the University G. d'Annunzio of Chieti to Feliciano Protasi. Rat skeletal alfa actin promoter was a kind gift from Dr. D. Yaffe D. Geenberg Departments of Cell biology Weizmann Institute, Rehovot Israel.

REFERENCES

Anderson AA, Treves S, Biral D, Betto R, Sandona D, Ronjat M, Zorzato F. 2003. The novel skeletal muscle sarcoplasmic reticulum JP-45 protein: molecular cloning, tissue distribution, developmental expression and interaction with α.1 subunit of the voltage gated calcium channel. J Biol Chem 278:39987-39992.

Bastianutto C, Clementi E, Codazzi F, Podini P, De Giorgi F, Rizzuto R, Meldolesi J, Pozzan T. 1995. Overexpression of calreticulin increases the Ca^{2+} capacity of rapidly exchanging Ca^{2+} stores and reveals aspects of their lumenal microenvironment and function. J Cell Biol 130:847-855.

Berchtold MW, Brinkmeier H, Muntener M. 2000. Calcium ion in skeletal muscle: its crucial role for muscle function, plasticity, and disease. Physiol. Rev. 80:1215-1265.

Caswell AH, Brandt NR, Brunschwig JP, Purkerson S. 1991. Localization and partial characterization of the oligomeric disulfide-linked molecular weight 95,000 protein (triadin)which binds the ryanodine and dihydropyridine receptors in skeletal muscle triadic vesicles. Biochemistry 30:7507-75013.

Costello B, Chadwick C, Saito A, Chu A, Maurer A, Fleischer S. 1986. Characterization of the junctional face membrane from terminal cisternae of sarcoplasmic reticulum. J Cell Biol 10:741-753.

Dinchuk JE, Henderson NL, Burn TC, Huber R, Ho SP, Link J, O'Neil KT, Focht RJ, Scully MS, Hollis JM, Hollis GF, Friedman PA. 2000. Aspartyl beta -hydroxylase (Asph) and an evolutionarily conserved isoform of Asph missing the catalytic domain share exons with junctin. J Biol Chem 275:39543-39554.

Divet A, Huchet-Cadiou C. 2002. Sarcoplasmic reticulum function in slow- and fast-twitch skeletal muscles from mdx mice. Pflügers Arch 44:634-643.

Divet A, Lompré AM, Huchet-Cadiou C. 2005. Effect of cyclopiazonic acid, an inhibitor of the sarcoplasmic reticulum Ca-ATPase, on skeletal muscles from normal and mdx mice. Acta Physiol Scand 184:173-186.

Ducreux S, Zorzato F, Müller CR, Sewry C, Muntoni F, Quinlivan R, Restagno G, Girard T, Treves S. 2004. Effect of ryanodine receptor mutations on IL-6 release and intracellular calcium homeostasis in human myotubes from malignant hyperthermia susceptible individuals and patients affected by central core disease. J Biol Chem 279:43838-43846.

Fan GC, Gregory KN, Zhao W, Park WJ, Kranias EG. 2004. Regulation of myocardial function by histidine-rich, calcium-binding protein. Am J Physiol Heart Circ Physiol 287:H1705-1711.

Fink RH, Stephenson DG, Williams DA. 1986. Calcium and strontium activation of single skinned muscle fibres of normal and dystrophic mice. J Physiol 373:513-525.

Franzini-Armstrong C, Jorgensen AO. 1994. Structure and development of E-C coupling units in skeletal muscle. Annu Rev Physiol 56:509-534.

Froemming GR, Pette D, Ohlendieck K. 1999. The 90-kDa junctional sarcoplasmic reticulum protein forms an integral part of a supramolecular triad complex in skeletal muscle. Biochem Biophys Res Commun 261:603-609.

Godt RE, Nosek TM. 1989. Changes of intracellular milieu with fatigue or hypoxia depress contraction of skinned rabbit skeletal and cardiac muscle. J Physiol 412:155-180.

Greenberg DS, Sunada Y, Campbell KP, Yaffe D, Nudel U. 1994. Exogenous Dp71 restores the levels of dystrophin associated proteins but does not alleviate muscle damage in mdx mice. Nat Genet 5:340-344.

Gronke RS, Welsch DJ, VanDusen WJ, Garsky VM, Sardana MK, Stern AM, Friedman PA. 1990. Partial purification and characterization of bovine liver aspartyl beta-hydroxylase. J Biol Chem 265:8558-8565.

Herrmann-Frank A, Richter M, Sarkozi S, Mohr U, Lehmann-Horn F. 1996. 4-Chloro-m-cresol, a potent and specific activator of the skeletal muscle ryanodine receptor. Biochim Biophys Acta 1289:31-40.

Hofmann SL, Goldstein JL, Orth K, Moomaw CR, Slaughter CA, Brown MS. 1989. Molecular cloning of a histidine-rich Ca2+-binding protein of sarcoplasmic reticulum that contains highly conserved repeated elements. J Biol Chem 264:18083-18090.

Hong CS, Kwak YG, Ji JH, Chae S, Kim do H. 2001. Molecular cloning and characterization of mouse cardiac junctate isoforms. Biochem Biophys Res Commun 289:882-887.

Huchet C, Leoty C. 1993. Calcium sensitivity of skinned ferret EDL, soleus, and cremaster fibers. Am J Physiol 264:R867-870.

Jones LR, Zhang L, Sanborn K, Jorgensen AO, Kelley J. 1995. Purification, primary structure, and immunological characterization of the 26-kDa calsequestrin binding protein (junctin) from cardiac junctional sarcoplasmic reticulum. J Biol Chem 270:30787-30796.

Jones LR, Suzuki YJ, Wang W, Kobayashi YM, RameshV, Franzini-Armstrong C, Cleemann L, Morad M. 1998. Regulation of Ca^{2+} signaling in transgenic mouse cardiac myocytes overexpressing calsequestrin J Clin Invest 101:1385-1393.

Kim E, Shin DW, Hong CS, Jeong D, Kim do H., Park WJ. 2003. Increased Ca^{2+} storage capacity in the sarcoplasmic reticulum by overexpression of HRC (histidine-rich Ca^{2+} binding protein). Biochem Biophys Res Commun 300:192-196.

Knollmann BC, Knollmann-Ritschel BE, Weissman NJ, Jones LR, Morad M. 2000. Remodelling of ionic currents in hypertrophied and failing hearts of transgenic mice overexpressing calsequestrin. J Physiol 525:483-498.

Lamb GD, Stephenson DG. 1990. Control of calcium release and the effect of ryanodine in skinned muscle fibres of the toad. J Physiol 423:495-517.

MacLennan DH, Wong PT. 1971. Isolation of a calcium-sequestering protein from sarcoplasmic reticulum. Proc Natl Acad Sci USA 68:1231-1235.

MacLennan DH. 2000. Ca2+ signaling and muscle disease. Eur J Biochem 267:5291-5297

Marty I, Robert M, Villaz M, De Jongh K, Lai Y, Catterall WA, Ronjat M. 1994. Biochemical

evidence for a complex involving dihydropyridine receptor and ryanodine receptor in triad junctions of skeletal muscle. Proc Natl Acad Sci U S A 91:2270-2274.

Melzer W, Herrmann-Frank A, Luttgau HC. 1995. The role of Ca2+ ions in excitation-contraction coupling of skeletal muscle fibres. Biochim Biophys Acta 1241:59-116.

Miller SL, Currie S, Loughrey CM, Kettlewell S, Seidler T, Reynolds DF, Hasenfuss G, Smith GL. 2005. Effects of calsequestrin over-expression on excitation-contraction coupling in isolated rabbit cardiomyocytes. Cardiovasc Res 67:667-677.

Mitchell RD, Volpe P, Palade P, Fleischer S. 1983. Biochemical characterization, integrity, and sidedness of purified skeletal muscle triads. J Biol Chem 258:9867-9877.

Nakai J, Dirksen RT, Nguyen HT, Pessah IN, Beam KG, Allen PD. 1996. Enhanced dihydropyridine receptor channel activity in the presence of ryanodine receptor. Nature 380:72-75.

Rios E, Ma JJ, Gonzalez A. 1991. The mechanical hypothesis of excitation-contraction (EC) coupling in skeletal muscle. J Muscle Res Cell Motil 12:127-135.

Palade P. 1987 Drug-induced Ca2+ release from isolated sarcoplasmic reticulum. III. Block of Ca^{2+}-induced Ca^{2+} release by organic polyamines. J Biol Chem 262:6135-6141.

Saito A, Seiler S, Chu A, Fleischer S. 1984. Preparation and morphology of sarcoplasmic reticulum terminal cisternae from rabbit skeletal muscle. J Cell Biol 99:875-885.

Sato Y, Ferguson DG, Sako H, Dorn GW, Kadambi VJ, Yatani A, Hoit BD, Walsh RA, Kranias EG. 1998. Cardiac-specific overexpression of mouse cardiac calsequestrin is associated with depressed cardiovascular function and hypertrophy in transgenic mice. J Biol Chem 273:28470-28477.

Schiaffino S, Reggiani C. 1996. Molecular diversity of myofibrillar proteins: gene regulation and functional significance. Physiol Rev 76:371-423.

Takeshima H, Shimuta M, Komazaki S, Ohmi, K, Nishi M, Iino M, Miyata A, Kangawa K. 1998. Mitsugumin 29, a novel synaptophysin family member from the triad junction in skeletal muscle. Biochem J 331:317-322.

Takeshima H, Komazaki S, Nishi M, Iino M, Kangawa K. 2000. Junctophilins: a novel family of junctional membrane complex proteins. Mol Cell 6:11-22.

Treves S, Feriotto G, Moccagatta L, Gambari R, Zorzato F. 2000. Molecular cloning, expression, fuctional characterization, chromosomal localization and gene structure of junctate a novel integral calcium binding protein of sarco(endo)plasmic reticulum membrane J Biol Chem 275:39555-39568.

Treves S, Franzini-Armstrong C, Moccagatta L, Arnoult C, Grasso C, Schrum A, Ducreux S, Zhu MX, Mikoshiba K, Girard T, Smida-Rezgui S, Ronjat M, Zorzato F. 2004. Junctate is a key element in calcium entry induced by activation of InsP3 receptors and/or calcium store depletion. J Cell Biol 166:537-548.

Wang QP, VanDusen WJ, Petroski CJ, Garsky VM, Stern AM Friedman PA. 1991. Bovine liver aspartyl beta-hydroxylase. Purification and characterization. J Biol Chem 266:14004-14010.

Warren GB, Toon PA, Birdsall NJ, Lee AG, Metcalfe JC. 1974. Reconstitution of a calcium pump

using defined membrane components. Proc Natl Acad Sci USA 71:622-626.

Xu W, Longo FJ, Wintermantel MR, Jiang X, Clark RA, DeLisle S. 2000. Calreticulin modulates capacitative Ca^{2+} influx by controlling the extent of inositol 1,4,5-trisphosphate-induced Ca2+ store depletion. J Biol Chem 275:36676-36682.

Zhang L, Kelley J, Schmeisser G, Kobayashi YM, Jones LR. 1997. Complex formation between junctin, triadin, calsequestrin, and the ryanodine receptor. Proteins of the cardiac junctional sarcoplasmic reticulum membrane. J Biol Chem 272:23389-23397.

Zorzato F, Salviati G, Facchinetti T, Volpe P. 1985. Doxorubicin induces calcium release from terminal cisternae of skeletal muscle. A study on isolated sarcoplasmic reticulum and chemically skinned fibers. J Biol Chem 260:7349-7355.

Zorzato F, Scutari E, Tegazzin V, Clementi E, Treves S. 1993. Chlorocresol: an activator of ryanodine receptor-mediated Ca^{2+} release. Mol Pharmacol 44:1192-1201.

Zorzato F, Anderson AA, Ohlendieck K, Froemming G, Guerrini R, Treves S. 2000. Identification of a novel 45 kDa protein (JP-45) from rabbit sarcoplasmic reticulum junctional face membrane. Biochem J 351:537-543.

FIGURE LEGENDS

Figure 1: Structure of the transgene, identification of transgenic mice and validity of junctate transgenic animal model. A - Schematic representation and restriction map of junctate transgene construct. The microinjected fragment was composed of the human junctate cDNA associated to α-actin promoter and a polyadenylation signal sequence. Arrows indicate forward (F) and reverse (R) primers used for PCR amplification experiments; the solid bar indicates cDNA sequence of the probe used for Southern blot analysis. B - Genotypic characterization of wild type (WT) and transgenic (TG) mice. Genomic DNA was isolated from mice amplified by PCR with two sets of primers specifically designed to amplify human junctate cDNA. C - Southern blot analysis of genomic DNA isolated from tail biopsies of homozygous (HO), heterozygous (HE) and wild type (WT) mice. 1 µg genomic DNA was digested with *HindIII*. The fragments were separated on a 1% agarose gel, transferred onto a nylon membrane and hybridized with human junctate specific cDNA probe overnight at 42°C. The next day the membrane was washed at high stringency (0.2 XSSCP, 0.1% SDS, 65°C) and hybridizing bands were visualized by autoradiography. D-Twenty micrograms of total SR isolated from the skeletal muscles of wild type (WT) and transgenic mice (TG) were separated in a 10% SDS PAG, blotted onto nitrocellulose and stained with Ponceau Red (left lanes) or with polyclonal anti-human junctate Abs (right lane, 0.5 µg/ml in TBST) followed by protein G- peroxidase (1:50000). Immunopositive bands were visualized by chemiluminescence (right).). Only the SR from TG mice contained an immunoreactive band recognized by the Abs. E-Competition experiments. Twenty micrograms of total SR isolated from the skeletal muscles of transgenic mice were separated on a 10% SDS PAG, blotted onto nitrocellulose and probed with polyclonal anti-junctate antibodies (0.5 µg/ml final concentration) pre-incubated with 0, 15 and 25 µg of the MAP peptide used to raise the antibodies. Blots were subsequently incubated with protein G-peroxidase (1:50000). Immunopositive bands were visualized by chemiluminescence

Figure 2: Calcium homeostasis in isolated myotubes from normal and junctate-over-expressing mice. A and B: Calcium imaging was performed as described in the Materials and Methods section on fura-2 loaded myotubes. Addition of 600 µM 4-CmC (traces in panel A) resulted in a rapid and transient increase of the cytoplasmic [Ca^{2+}], which was significantly larger in cells from TG (….) compared to WT (__); panel B shows that the average (mean ± S.E.M.) peak Ca^{2+} increase in normal and junctate over-expressing myotubes is significantly different**. C and D:** Calcium influx in myotubes depleted of intracellular Ca^{2+}-store by incubation with 1 mM EGTA, was initiated by addition of 2 mM Ca^{2+}. Panel C shows a representative trace obtained from a single cell; the peak influx was larger in TG myotubes (….) compared to WT (___); panel D shows that the mean (± S.E.M.) Ca^{2+} influx is significantly larger in junctate over-expressing myotubes

Figure 3: Maximal SR Ca^{2+} loading capacity. A - The maximal Ca^{2+} loading capacity was studied in SR microsomes from wild type and transgenic mice, as described in Experimental procedures. 50

µg/mL protein were loaded with pulses of 10 nmoles $CaCl_2$, then Ca^{2+} release was induced by the application of the Ca^{2+} ionophore A23187 (5 µg/mL). B - The maximal amount of Ca^{2+} loading was determined and expressed as the percentage of Ca^{2+} loading obtained in SR preparations from WT mice. C - Total Ca^{2+} release induced by the ionophore A23187 (5 µg/mL) was determined and expressed as the percentage of release obtained in SR preparations from WT mice. Values are mean ±S.E.M. ; n= is the number of SR microsome preparations. *** P<0.001 vs. WT mice.

Figure 4: Comparison of Ca^{2+} release induced by 4-chloro-*m*-cresol in SR from wild type and transgenic mice. A- Ca^{2+} release induced by the application of 4-chloro-*m*-cresol (4-CmC) was studied in SR microsomes from WT and TG mice, as described in Experimental procedures. Microsomes (50 µg/mL) were loaded with pulses of 10 nmoles $CaCl_2$ and Ca^{2+} release was triggered by the application of 4-CmC. The total amount of Ca^{2+} accumulated by the SR was released by the application of Ca^{2+} ionophore A23187 (5 µg/mL). B- Dose dependent 4-CmC-induced Ca^{2+} release relationships in SR microsomes from wild type (_) and transgenic (_) mice**:** dose-response curves to 4-CmC-induced Ca^{2+} release were generated on SR microsomes from wild type (n=6) and transgenic mice (n=5). The extent of Ca^{2+} release was measured. Values are mean±S.E.M.; n is the number of SR microsomal preparations corresponding to a mixture of muscles from 3 mice. * P<0.05 vs. WT mice.

Figure 5: Analysis of SR Ca^{2+}-ATPase expression and luminal Ca^{2+} binding protein in SR from wild type and transgenic mice. Top panels: Anti-SERCA1 and anti-SERCA2 antibodies immunostaining of SR microsome preparations from WT and TG mice. Relative expression levels of Ca^{2+}-ATPase were estimated by densitometry analysis and normalized to WT data. Values are mean±S.E.M.; n = number of different SR microsome preparations corresponding to a mix of muscles from 3 mice. *ns* non significant difference vs. WT mice.
Bottom panels: Anti-calsequestrin, anti-sarcalumenin and anti-calreticulin antibodies immunostaining of SR microsome preparations from WT and TG mice. Relative expression levels were estimated by densitometry analysis and normalized to WT data. Values are means±S.E.M ; n = number of SR microsome preparations corresponding to a mix of muscles from 3 mice. *ns* non significant difference vs. WT mice.

Figure 6: Overall architecture of EDL muscle fibers in WT (panel A) and TG (panel B) mice. The ultrastructural analysis performed by EM indicates that junctate over-expression does not induce drastic alterations in the general organization and architecture of muscle fibers. Myofibrils appear to be well aligned with one another (see Z lines). Triads are correctly positioned and orientated at the transition between I and A bands (small arrows) and their appearance (see enlarged details) seems normal. The only noticeable alteration detected at the EM analysis concerns the content of mitochondria (empty attows) in the EDL muscle, since in the TG mice we found a large increase in their number when compared to WT (see Table 3, column V).

Figure 7: Tension/pSr relationships in Triton skinned fibers. Tension/pSr relationships were studied in slow- (soleus) and fast-twitch (*extensor digitorum longus*, EDL) muscles from WT and TG mice. Curves were fitted using the modified Hill equation (see Experimental procedures and Table 4 for values). Values are mean±S.E.M.; n = number of fibers.

Figure 1

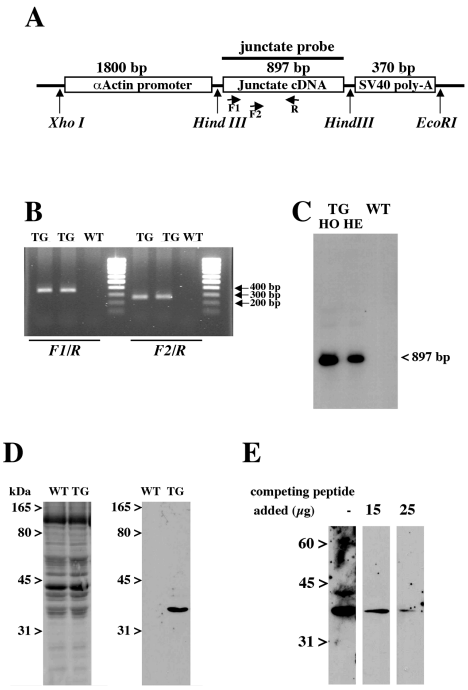

Figure 2

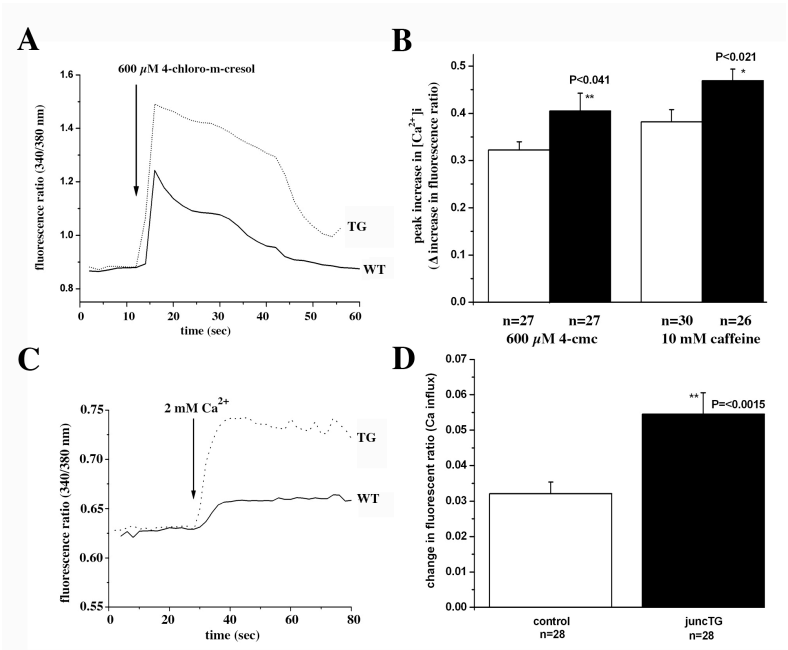

Figure 3

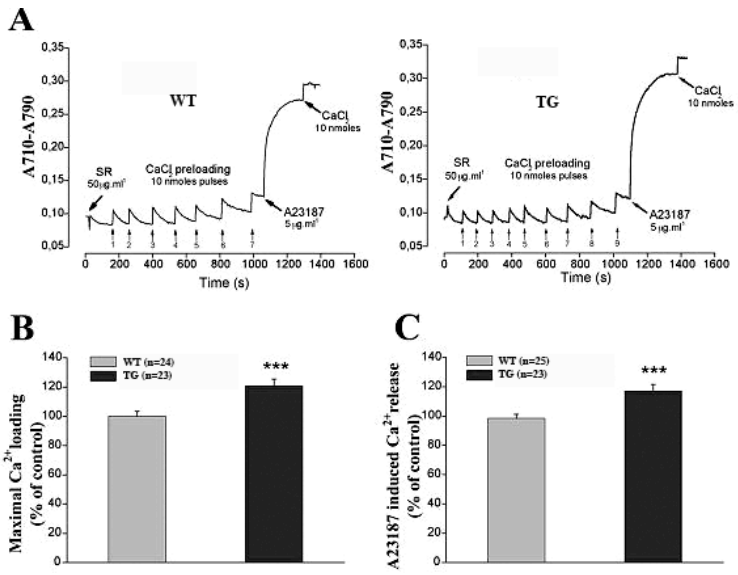

Figure 4

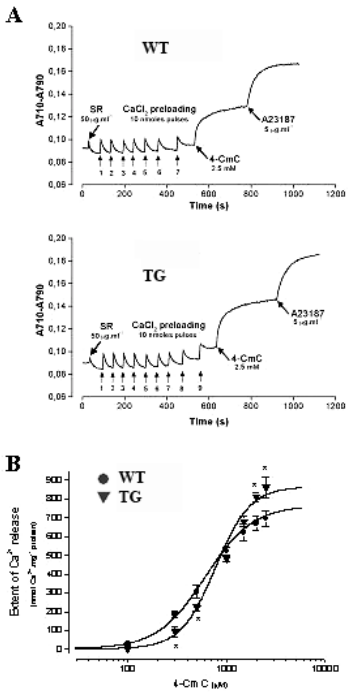

Figure 5

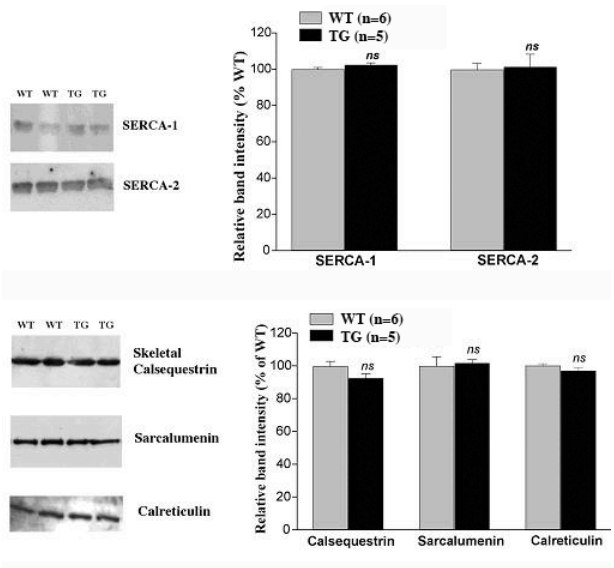

Figure 6

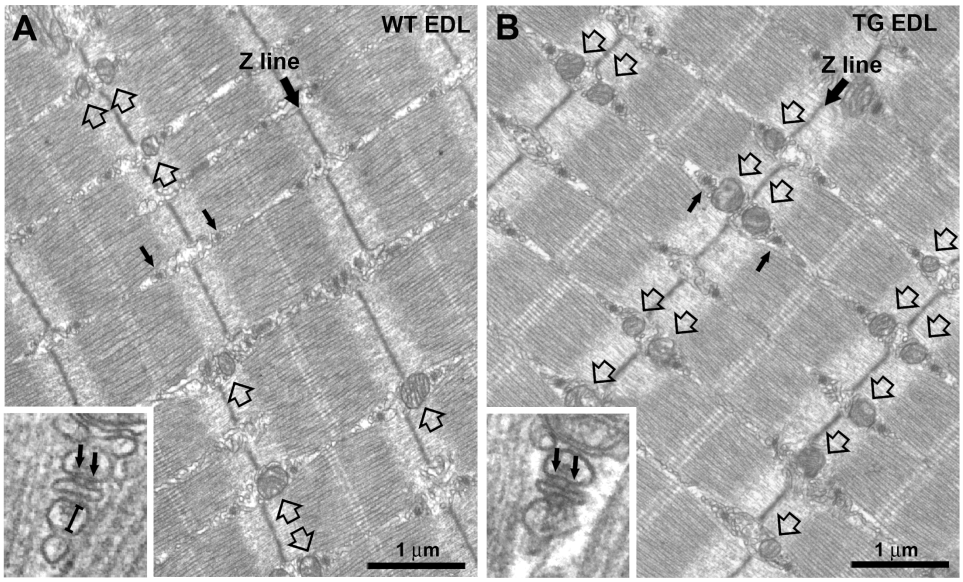

Figure 7

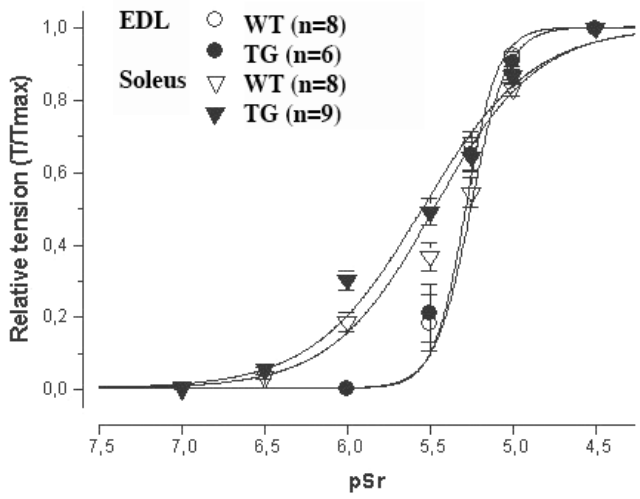
EDL
WT (n=8)
TG (n=6)
Soleus
WT (n=8)
TG (n=9)
Relative tension (T/Tmax)
1,0
0,8
0,6
0,4
0,2
0,0
7,5
7,0
6,5
6,0
5,5
5,0
4,5
pSr